A WIND ENERGY CONVERSION SYSTEM WITH REACTIVE POWER MANAGEMENT CAPABILITIES FOR POWER GRID

[1]J. Swetha, [2]K. Dinesh kumar Reddy, [3]M.Venkata Kishore

[1]Student, [2,3]Assistant Professor
Department of Electrical & Electronics Engineering
Balaji Institute of Technology & Sciences, Lingapuram, Andhra Pradesh, India.

***Abstract*: This project deals with the operation of doubly fed induction generator (DFIG) with an integrated active filter capabilities using grid-side converter (GSC). The main contribution of this work lies in the control of GSC for supplying harmonics in addition to its slip power transfer. The rotor-side converter (RSC) is used for attaining maximum power extraction and to supply required reactive power to DFIG. This wind energy conversion system (WECS) works as a static compensator (STATCOM) for supplying harmonics even when the wind turbine is in shut- down condition. Control algorithms of both GSC and RSC are presented in detail. The proposed DFIG-based WECS is simulated using MATLAB/Simulink. A prototype of the proposed DFIG- based WECS is developed using a digital signal processor (DSP). Simulated results are validated with test results of the developed DFIG for different practical conditions, such as variable wind speed and unbalanced/single phase loads.**

1. Introduction

the conventional energy sources such as coal, oil, and gas are limited in nature. Now, there is a need for renew- able energy sources for the future energy demand. The other main advantages of this renewable source are eco-friendliness and unlimited in nature. Due to technical advancements, the cost of the wind power produced is comparable to that of conventional power plants. Therefore, the wind energy is the most preferred out of all renewable energy sources. In the initial days, wind turbines have been used as fixed speed wind turbines with squirrel cage induction generator and capacitor banks. Most of the wind turbines are fixed speed because of their simplicity and low cost. By observing wind turbine characteristics, one can clearly identify that for extracting maximum power, the machine should run at varying rotor speeds at different wind speeds. Using modern power electronic converters, the machine is able to run at adjustable speeds. Therefore, these variable speed wind turbines are able to improve the wind energy production. Out of all variable speed wind turbines, doubly fed induction generators (DFIGs) are preferred because of their low cost. The other advantages of this DFIG are the higher energy output, lower converter rating, and better utilization of generators. These DFIGs also provide good damping performance for the weak grid. Independent control of active and reactive power is achieved by the decoupled vector control algorithm presented in [10] and [11]. This vector control of such system is usually realized in synchronously rotating reference frame oriented in either volt- age axis or flux axis. In this work, the control of rotor-side converter (RSC) is implemented in voltage-oriented reference frame.

TABLE I
[35] CURRENT DISTORTION LIMITS FOR GENERAL DISTRIBUTION SYSTEMS IN TERMS OF INDIVIDUAL HARMONICS ORDER (ODD HARMONICS) [35]

I_{sc}/I_L	<11	11 ≤ h ≤17	17 ≤ h ≤ 23	23 ≤ h ≤ 35	35 ≤ h	TDD
< 20	4.0	2.0	1.5	0.6	0.3	5.0
20 < 50	7.0	3.5	2.5	1.0	0.5	8.0
50 < 100	10	4.5	4.0	1.5	0.7	12
100 < 1000	12	5.5	5.0	2.0	1.0	15.0
> 1000	15.0	7.0	6.0	2.5	1.4	20.0

As the wind penetration in the grid becomes significant, the use of variable speed WECS for supplementary jobs such as power smoothen- ing and harmonic mitigation are compulsory in addition to its power generation. This power smoothening is achieved by including super magnetic energy storage systems as proposed in. The other auxiliary services such as reactive power requirement and transient stability limit are achieved by includ- ing static compensator (STATCOM) in. A distribution STATCOM (DSTATCOM) coupled with fly-wheel energy storage system is used at the wind farm for mitigating harmonics and frequency disturbances [16]. However, the authors have used two more extra converters for this purpose. A super capac- itor energy storage system at the dc link of unified power quality conditioner (UPQC) is proposed in [17] for improving power quality and reliability. In all above methods [15]–[17], the authors have used separate converters for compensating the har- monics and also for controlling the reactive power. However, in later stages, some of the researchers have modified the control algorithms of already existed DFIG converters for mitigating the power quality problems and reactive power compensation [18]–[26]. The harmonics compensation and reactive power control are achieved with the help of existing RSC [18]–[23].

2. SYSTEM CONFIGURATION AND OPERATING PRINCIPLE

schematic diagram of the proposed DFIG- based WECS with integrated active filter capabilities. In DFIG, the

stator is directly connected to the grid as shown in Fig. 1. Two back-to-back connected voltage source converters (VSCs) are placed between the rotor and the grid. Nonlinear loads are connected at PCC as shown in Fig. 1. The proposed DFIG works as an active filter in addition to the active power gen- eration similar to normal DFIG. Harmonics generated by the nonlinear load connected at the PCC distort the PCC voltage. These nonlinear load harmonic currents are mitigated by GSC control, so that the stator and grid currents are harmonic-free. RSC is controlled for achieving maximum power point tracking (MPPT) and also for making unity power factor at the stator side using voltage-oriented reference frame. Synchronous reference frame (SRF) control method is used for extracting the fundamental component of load currents for the GSC control.

a new control algorithm for GSC is pro- posed for compensating harmonics produced by nonlinear loads using an indirect current control. RSC is used for control- ling the reactive power of DFIG. The other main advantage of proposed DFIG is that it works as an active filter even when the wind turbine is in shutdown condition. Therefore, it compensates load reactive power and harmonics at wind turbine stalling case. Both simulation and experimental peformances of the proposed integrated active filter-based DFIG are presented in this work. The dynamic performance of the proposed DFIG is also demonstrated for varying wind speeds and changes in unbalanced nonlinear loads at point of common coupling (PCC).

3. DESIGN OF DFIG-BASED WECS

Selection of ratings of VSCs and dc-link voltage is very much important for the successful operation of WECS. The ratings of DFIG and dc machine used in this experimental system are given in Appendix. In this section, a detailed design of VSCs and dc-link voltage is discussed for the experimental system used in the laboratory.

Normally, the dc-link voltage of VSC must be greater than twice the peak of maximum phase voltage. The selection of dc- link voltage depends on both rotor voltage and PCC voltage. While considering from the rotor side, the rotor voltage is slip times the stator voltage. DFIG used in this prototype has stator to rotor turns ratio as 2:1. Normally, the DFIG operating slip is ±0.3. So, the rotor voltage is always less than the PCC voltage.

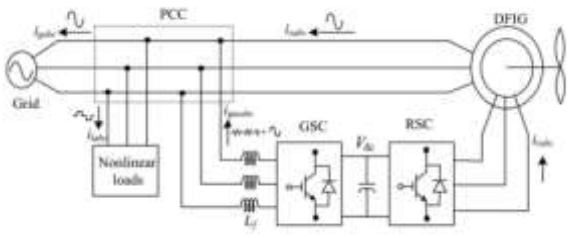

Fig. 3.1. Proposed system configuration

the line voltage at the PCC. Maximum modula- tion index is selected as 1 for linear range. The value of dc-link voltage.

$$V_{\mathrm{dc}} \geq \frac{2\sqrt{2}}{\sqrt{3} * m} V_{ab}$$

3.1 Selection of VSC Rating:

The DFIG draws a lagging volt-ampere reactive (VAR) for its excitation to build the rated air gap voltage. It is calculated from the machine parameters that the lagging VAR of 2 kVAR is needed when it is running as a motor. In DFIG case, the oper- ating speed range is 0.7 to 1.3 p.u. Therefore, the maximum slip.

$$S_{\mathrm{rated}} = \sqrt{P_{r\max}^2 + Q_{r\max}^2}.$$

3.2 Design of Interfacing Inductor:

dc-link voltage, and switching frequency of GSC. Maximum possible GSC line currents are used for the calculation. Maximum line current depends upon the maximum power and the line voltage at GSC. The maximum possible power in the GSC is the slip power. In this case, the slip power is 1.5 kW. Line voltage.

$$L_i = \frac{\sqrt{3}\, \mathrm{m} v_{\mathrm{dc}}}{12 a f_m \Delta i_{\mathrm{gsc}}}$$

$$= \frac{\sqrt{3} \times 1 \times 375}{12 \times 1.5 \times 10\,000 \times 0.25 \times 3.76} = 3.8\ \mathrm{mH}.$$

4. CONTROL STRATEGY:

Control algorithms for both GSC and RSC are presented in this section. Complete control schematic is given in Fig. 2. The control algorithm for emulating wind turbine characteris- tics using dc machine and Type A chopper.

4.1 Control of RSC:

main purpose of RSC is to extract maximum power with independent control of active and reactive powers. Here, the RSC is controlled in voltage-oriented reference frame. Therefore, the active and reactive powers are controlled by con- trolling direct and quadrature axis rotor currents.

This can be achieved by running the DFIG at a rotor speed for a particular wind speed. Therefore, the outer loop is selected as a speed controller for achieving direct axis reference rotor current.

$$i_{\mathrm{dr}}^{*}(k) = i_{\mathrm{dr}}^{*}(k-1) + k_{\mathrm{pd}}\left\{\omega_{\mathrm{er}}(k) - \omega_{\mathrm{er}}(k-1)\right\} + k_{\mathrm{id}}\omega_{\mathrm{er}}(k)$$

estimated by optimal tip speed ratio control for a particular wind speed.

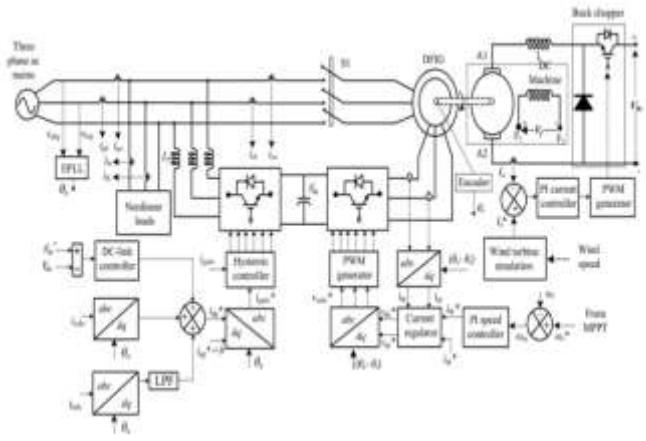

The tuning of PI controllers used in both RSC and GSC are achieved using Ziegler Nichols method. Initially. selected such that the stator reactive power Q s selected for injecting the required reactive power.

$$i_{dr} = 2/3 \begin{bmatrix} i_{ra} \sin \theta_{slip} + i_{rb} \sin(\theta_{slip} - 2\pi/3) \\ + i_{rc} \sin(\theta_{slip} + 2\pi/3) \end{bmatrix}$$

$$i_{qr} = 2/3 \begin{bmatrix} i_{ra} \cos \theta_{slip} + i_{rb} \cos(\theta_{slip} - 2\pi/3) \\ + i_{rc} \cos(\theta_{slip} + 2\pi/3) \end{bmatrix}$$

$$v^*_{ra} = v^*_{dr} \sin \theta_{slip} + v^*_{qr} \cos \theta_{slip}$$

$$v^*_{rb} = v^*_{dr} \sin(\theta_{slip} - 2\pi/3) + v^*_{qr} \cos(\theta_{slip} - 2\pi/3)$$

$$v^*_{rc} = v^*_{dr} \sin(\theta_{slip} + 2\pi/3) + v^*_{qr} \cos(\theta_{slip} + 2\pi/3).$$

6. Using Model-1 DFIG based WECS at fixed wind speed of 10.6m/s.(rotor speed of 1750 rpm).

Simulated output waveforms for the proposed model-1 DFIG- based WECS at fixed wind speed of 10.6 m/s with a rotor speed of 1750 rpm. At this case As the proposed DFIG is operating at MPPT, the reference speed of the DFIG is selected as 1750 rpm. The load currents are observed to be nonlinear in nature. The GSC is supplying required harmonics currents to the load for making grid currents (i_{gabc}) and stator currents (i_{sabc}) balanced and sinusoidal. Fig. 5.2 also shows the stator power (P_s), GSC power (P_{gsc}), load power (P_l), and grid power (P_g). At above synchronous speed, the power flow is from the GSC to PCC, so the GSC power is shown as positive.

Total power produced by the DFIG is the sum of stator power (P_s) and GSC power (P_{gsc}). After feeding power to the load (P_l), the remaining power is fed to the grid (P_g). Fig. 5.1 (a)–(d) shows harmonic spectra and waveforms of grid current (i_{ga}), load current (i_{la}), stator current (i_{sa}), and grid voltage (v_{ga}), respectively. From these harmonic spectra, one can understand that grid current and stator current THDs are less than 5% as per IEEE-519 standard [35] limits given in Table I.

7. Results:

7.1 Simulation circuit diagram of proposed Model-1 DFIG based WECS at fixed wind speed of 10.6m/s.(rotor speed of 1750 rpm).

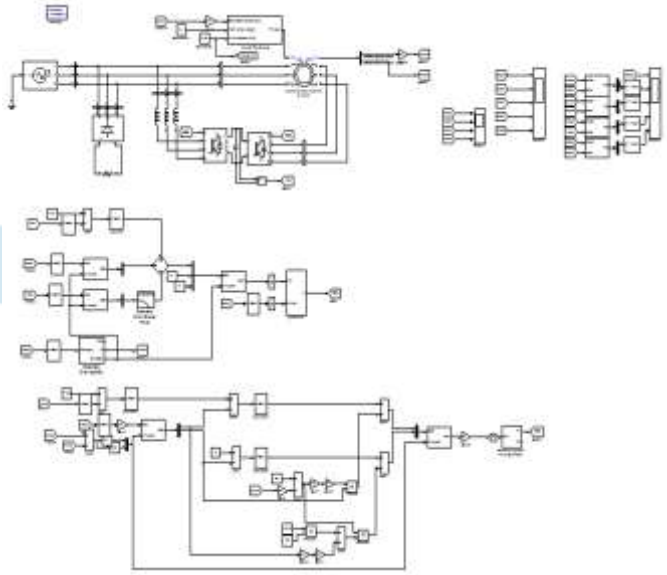

Fig: 7.1 Simulated circuit diagram of the proposed model-1 DFIG-based WECS at fixed wind speed of 10.6 m/s (rotor speed of 1750 rpm).

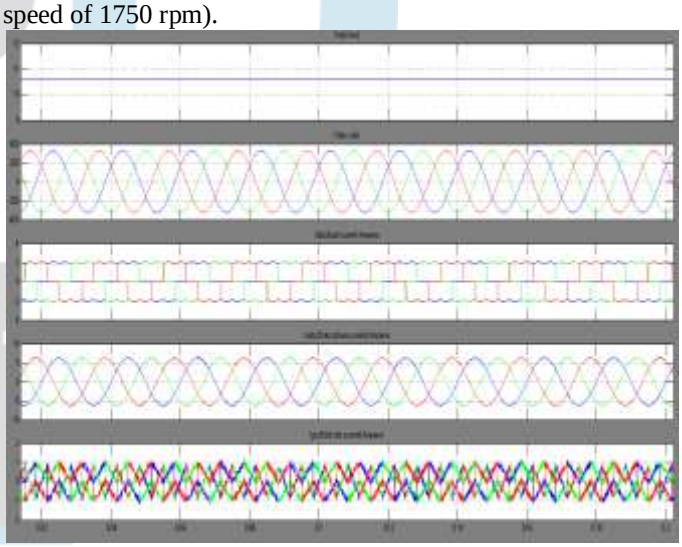

Fig: 7.2 Simulated performance of the proposed DFIG-based WECS at fixed wind speed of 10.6 m/s (rotor speed of 1750 rpm).(a)ω_r (b) V_{abc} (c) I_{labc} (d) I_{sabc} (e) V_{abc} (f) I_{gsc} (g) I_{gabc} (h) P_s (i) P_{gsc} (j) P_l (k) P_g

7.2 Simulation circuit diagram of proposed Model-2 DFIG based WECS
Working as a Statcom at zero wind speed.

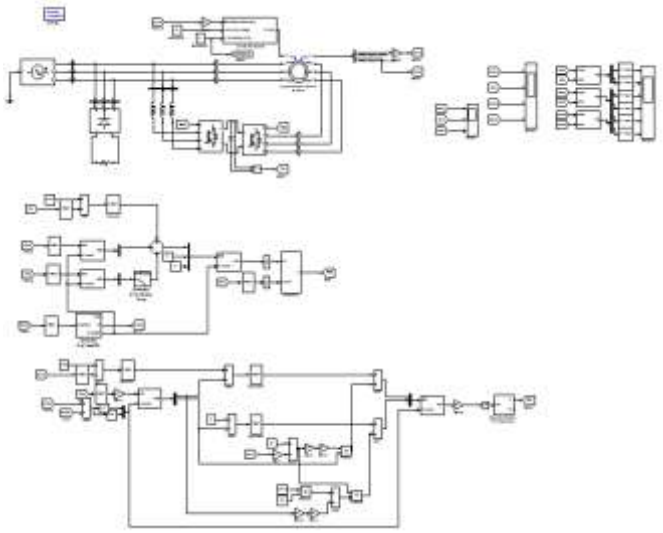

7.3 Simulated circuit diagram of the proposed model-2 DFIG-based WECS working as a STATCOM at zero wind speed.

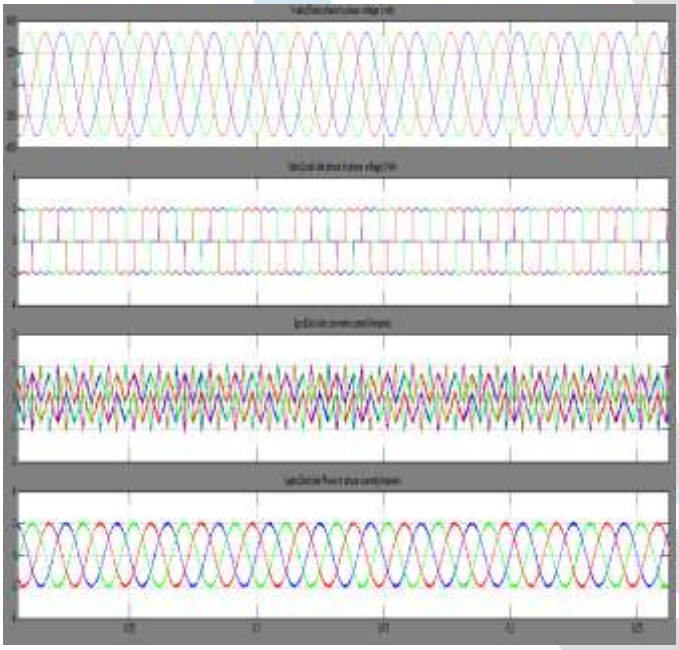

7.4. Simulated performance of the proposed model-2 DFIG-based WECS working as a STATCOM at zero wind speed (a) V_{abc} (b) I_{labc} (c) I_{gsc} (d) I_{gabc} (e) P_l (f) q_l (g) P_g (h) q_g (i) P_{gsc} (j) q_{gsc}

7.3 Simulation circuit diagram of proposed Model-7 DFIG based WECS
at fixed wind speed of 10.6m/s.(rotor speed of 1750 rpm) with Torque
load model.

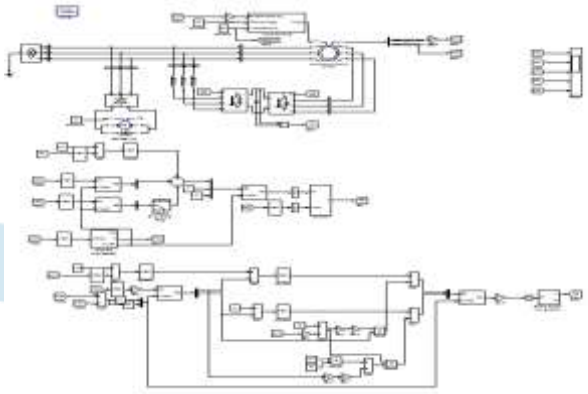

7.5 Simulated circuit diagram of the proposed model-6 DFIG-based WECS for fixed
wind speed of 10.6m/s.(rotor speed of 1750 rpm) with Torque load model.

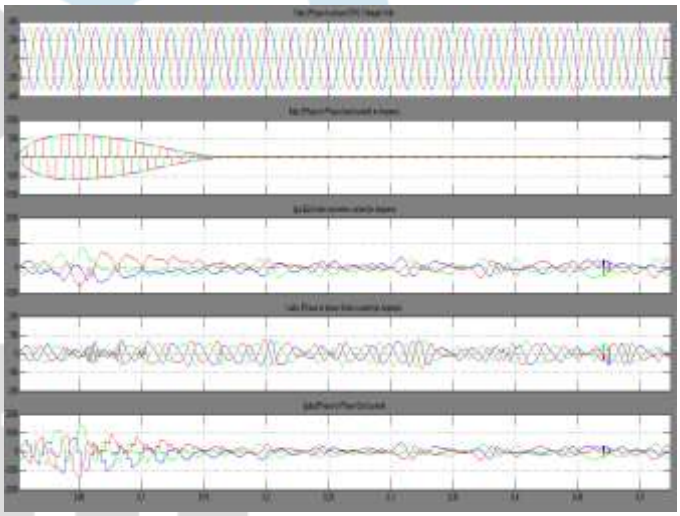

7.6 Shows the dynamic performance of this proposed DFIG-based WECS at fixe wind speed of 10.6m/s.(rotor speed of 1750 rpm) with Torque load model. (a)V_{abc} (b)i_{labc} (c)i_{gsc} (d) i_{sabc} (e)i_{gabc}

CONCLUSION

The GSC control algorithm of the proposed DFIG has been modified for supplying the harmonics and reactive power of the local loads. In this proposed DFIG, the reactive power for the induction machine has been supplied from the RSC and the load reactive power has been supplied from the GSC. The decoupled control of both active and reactive powers has been achieved by RSC control. The proposed DFIG has also been verified at wind turbine stalling condition for compensating harmonics and reactive power of local loads. This proposed DFIG-based WECS with an integrated active filter has been simulated using MATLAB/Simulink environment, and the simulated results are verified with test results of the developed prototype of this WECS.

Steady-state performance of the proposed DFIG has been demonstrated for a wind speed. Dynamic performance of this proposed GSC control algorithm has also been verified for the variation in the wind speeds and for local nonlinear load.

REFERENCES

[1] R. Adapa, "High-wire act: HVDC technology: The state of the art,"IEEE Power Energy Mag., vol. 10, no. 6, pp. 18–29, Nov. 2012.
[2] M. Klein, G. Rogers, and P. Kundur, "A fundamental study of inter area oscillations in power systems," IEEE Trans. Power Syst., vol. 6, no. 3, pp. 914–921, Aug. 1991.
[3] R. Sadikovic, "Use of FACTS devices for power flow control and damping of oscillations in power systems," Ph.D. dissertation, ETHZurich, Zurich, Switzerland, 2006.
[4] M. Aboul-Ela, A. Sallam, J. McCalley, and A. Fouad, "Damping controller design for power system oscillations using global signals," IEEE Trans. Power Syst., vol. 11, no. 2, pp. 767–773, May 1996.
[5] P. Kundur, N. Balu, and M. Lauby, Power System Stability and Control. New York: McGraw-Hill, 1994, vol. 141.
[6] D. Jovcic, L. A. Lamont, and L. Xu, "VSC transmission model for analytical studies," in Proc. IEEE Power Energy Soc. Gen. Meeting, 2003, pp. 1737–1742.
[7] J. Pan, R. Nuqui, K. Srivastava, T. Jonsson, P. Holmberg, and Y. Hafner, "AC grid with embedded VSC-HVDC for secure and efficient power delivery," presented at the IEEE Energy 2030, Atlanta, GA, USA, and Nov. 2008.
[8] B. P. X. Zhang and C. Rehtanz, Flexible AC Transmission Systems: Modeling and Control. Berlin, Germany: Springer-Verlag, 2006.
[9] G. Hug-Glanzmann, "Coordinated power flow control to enhance steady-state security in power systems," Ph.D. dissertation, Dept. Inf. Technol. Elect. Eng., ETH Zurich, Zurich, Switzerland, May 2008..
[10] H. Latorre, M. Ghandhari, and L. Söder, "Active and reactive power control of a VSC-HVDC," Elect. Power Syst. Res., vol. 78, pp. 1756–1763, Oct. 2008.
[11] R. Preece, A. Almutairi, O. Marjanovic, and J. Milanovic, "Damping of electromechanical oscillations by VSC-HVDC active power modulation with supplementary wams based modal lqg controller," presented at the IEEE Power Energy Soc. Gen. Meeting, San Diego, CA, USA, Jul. 2011.